Check for updates

*International Journal of Satellite Communications and Networking*

WILEY

SPECIAL ISSUE PAPER OPEN ACCESS

# SMTC Configuration and Window Adjustment Strategies for Beam Hopping in NR-NTN

Hee Wook Kim | Kyungrak Lee | Joon Gyu Ryu

Radio and Satellite Research Division, ETRI, Daejeon, Republic of Korea

**Correspondence:** Hee Wook Kim (prince304@etri.re.kr)

**Received:** 24 March 2026 | **Revised:** 24 June 2026 | **Accepted:** 27 June 2026

**Keywords:** beam hopping | nonterrestrial networks | NR synchronization | SMTC | satellite communications

## ABSTRACT

Beam hopping is an effective transmission strategy for nonterrestrial networks (NTNs), enabling satellites to allocate limited power and spectrum resources across different geographical regions over time. However, in NR-based NTN systems, beam hopping complicates synchronization monitoring because synchronization signal block (SSB) arrivals observed at a user equipment (UE) may be distributed across multiple disjoint time intervals within a beam hopping period. Under such conditions, the existing Synchronization Signal Block Measurement Timing Configuration (SMTC) framework, which was not designed to explicitly account for beam hopping-induced timing dispersion, may provide insufficient monitoring coverage. This paper investigates the limitations of the current SMTC mechanism in beam hopping NR-NTN systems and develops an analytical framework for characterizing SSB monitoring requirements. The analysis shows that the required number of SMTC configurations is governed by the number of illumination groups observed by the UE, and that the current configuration constraint may result in both incomplete timing-group coverage and residual window misalignment. To address these limitations, an enhanced SMTC monitoring framework is proposed, combining location-based configuration selection with timing-aware window adjustment. The proposed framework allows the network to maintain a larger candidate configuration pool while enabling the UE to activate only a capability-limited subset relevant to its location. Simulation results show that the proposed scheme improves SSB monitoring success probability across clustered and scattered beam hopping scenarios while clarifying the trade-off between monitoring performance and UE duty cycle. These results provide design insights for future NR-NTN evolution and practical beam hopping deployment.

## 1 | Introduction

Nonterrestrial networks (NTNs) have attracted significant attention as a key component of future wireless communication systems [1–4]. By integrating satellite platforms with terrestrial cellular infrastructures, NTNs can extend service coverage to remote, maritime, aerial, and disaster-affected areas where terrestrial deployment is impractical or cost-inefficient [1, 2]. The standardization of NR-based NTN architectures within the 3GPP framework has further accelerated the development of integrated satellite–terrestrial systems supporting broadband access and massive machine-type communications [2, 5, 6].

Beam hopping is an important transmission technique for improving spectral and power efficiency in multibeam satellite systems [7–9]. Instead of illuminating all beams simultaneously, the satellite activates a subset of beams over time according to a beam hopping schedule. This allows limited satellite resources to be concentrated on selected geographical regions and reused across different beams. While this operation improves resource utilization, it also changes the temporal structure of downlink signals observed at the user equipment (UE).

In NR systems, initial synchronization and cell identification are performed through the reception of synchronization signal blocks (SSBs), which include the primary synchronization signal,

This is an open access article under the terms of the Creative Commons Attribution License, which permits use, distribution and reproduction in any medium, provided the original work is properly cited.

© 2026 The Author(s). *International Journal of Satellite Communications and Networking* published by John Wiley & Sons Ltd.

the secondary synchronization signal, and the physical broadcast channel [10, 11]. To reduce receiver activity during SSB search and measurement, the Synchronization Signal Block Measurement Timing Configuration (SMTC) mechanism defines monitoring windows during which the UE activates its receiver [10].

In conventional terrestrial deployments, SSB arrival timings from relevant cells are relatively stable and can typically be covered by a small number of monitoring windows. In beam hopping NR-NTN systems, this assumption may no longer hold. SSB transmissions associated with different beams occur at different beam activation instants, and their arrival times at the UE are further shifted by propagation delay differences determined by satellite geometry and UE location. Consequently, SSB arrival opportunities may be distributed across multiple separated time intervals within a beam hopping period rather than concentrated in a compact timing region. A UE located near a beam boundary may therefore require several monitoring windows to capture SSBs from the serving and neighboring beams. However, the current NR SMTC framework supports only a limited number of SMTC configurations [5, 10]. This constraint can lead to incomplete monitoring coverage when the number of distinct arrival timing groups exceeds the number of configurations that can be activated.

Motivated by this limitation, this paper investigates synchronization monitoring in beam hopping NR-NTN systems. The objective is not to modify the physical-layer SSB detection procedure itself, but to improve the timing-domain monitoring framework so that SSB arrival opportunities created by beam hopping can be captured more reliably. In particular, we show that the monitoring requirement is governed by the number of illumination groups observed by the UE, rather than solely by the total timing spread. Based on this observation, we propose an enhanced SMTC monitoring framework that combines location-based configuration selection and adaptive window adjustment. The framework also considers network-side configuration management, gateway-assisted beam scheduling, UE capability constraints, and fallback operation under degraded assistance information.

The main contributions of this work are summarized as follows:

- We formulate the synchronization monitoring problem in beam hopping NR-NTN systems using an illumination-group abstraction. The analysis identifies the number of illumination groups observed at the UE as the key factor determining the required number of SMTC configurations.
- We propose a location-based SMTC configuration strategy in which the network maintains a candidate configuration pool, whereas the UE activates only a capability-limited subset relevant to its location. The strategy supports autonomous selection in idle or inactive mode and network-assisted configuration in connected mode.
- An adaptive SMTC window adjustment mechanism is introduced, which compensates for timing misalignment caused by differential propagation delay between beam reference points and the actual UE location.
- We develop an analytical and simulation-based evaluation framework that captures both timing-group coverage and window alignment effects. The results quantify the trade-off between SSB monitoring success probability and UE monitoring duty cycle across clustered and scattered beam hopping scenarios.
- We discuss practical integration aspects, including the interaction with beam hopping scheduling, gateway and RAN-side configuration management, UE capability constraints, and possible standardization paths for future NR-NTN evolution.

The remainder of this paper is organized as follows. Section 2 reviews the NR SMTC mechanism, beam hopping operation, and related work. Section 3 analyzes the limitations of the existing SMTC framework using an illumination-group–based timing model. Section 4 presents the proposed enhanced monitoring framework. Section 5 evaluates the monitoring performance and duty-cycle trade-off through simulation. Finally, Section 6 concludes the paper.

## 2 | Background and Related Work

### 2.1 | NR Synchronization and SMTC Mechanism

In NR, synchronization and cell identification are supported by SSB reception. Each SSB carries the primary synchronization signal, the secondary synchronization signal, and the physical broadcast channel, allowing the UE to obtain timing, frequency, and cell identity information required for initial access and mobility procedures [10, 11]. Since continuous SSB monitoring would increase receiver activity, NR defines the SMTC mechanism to restrict SSB search and measurement to configured time windows. An SMTC configuration specifies the timing properties of a monitoring occasion, including its periodicity, offset, and duration. During the configured window, the UE activates its receiver and performs SSB detection or measurement; outside the window, receiver activity can be reduced to save power [11].

This design is effective when the SSB arrival timings of relevant cells are sufficiently concentrated in time. In conventional terrestrial deployments, such an assumption is generally reasonable because the timing relationship among neighboring cells is comparatively stable. In NR-NTN, however, the timing relationship between transmission and reception is affected by satellite propagation delay and satellite movement. Although the current NR-NTN framework accounts for large absolute propagation delays through NTN-specific procedures, the SMTC configuration framework still assumes that a limited number of monitoring windows can cover the relevant SSB measurement occasions. The number of SMTC configurations is therefore constrained to a small set, with the current specification supporting up to four configurations [5, 10]. This constraint becomes important when beam hopping causes SSB arrival opportunities to be separated into multiple timing regions, as discussed next.

### 2.2 | Beam Hopping Operation and Timing Characteristics in NTN Systems

Beam hopping improves satellite resource utilization by activating different beams at different time instants according to a predefined or dynamically updated hopping schedule. During



15420981, 0, Downloaded from https://onlinelibrary.wiley.com/doi/10.1002/sat.70073 by Hee Wook Kim - Electronics and Telecommunications , Wiley Online Library on [09/07/2026]. See the Terms and Conditions (https://onlinelibrary.wiley.com/terms-and-conditions) on Wiley Online Library for rules of use; OA articles are governed by the applicable Creative Commons License

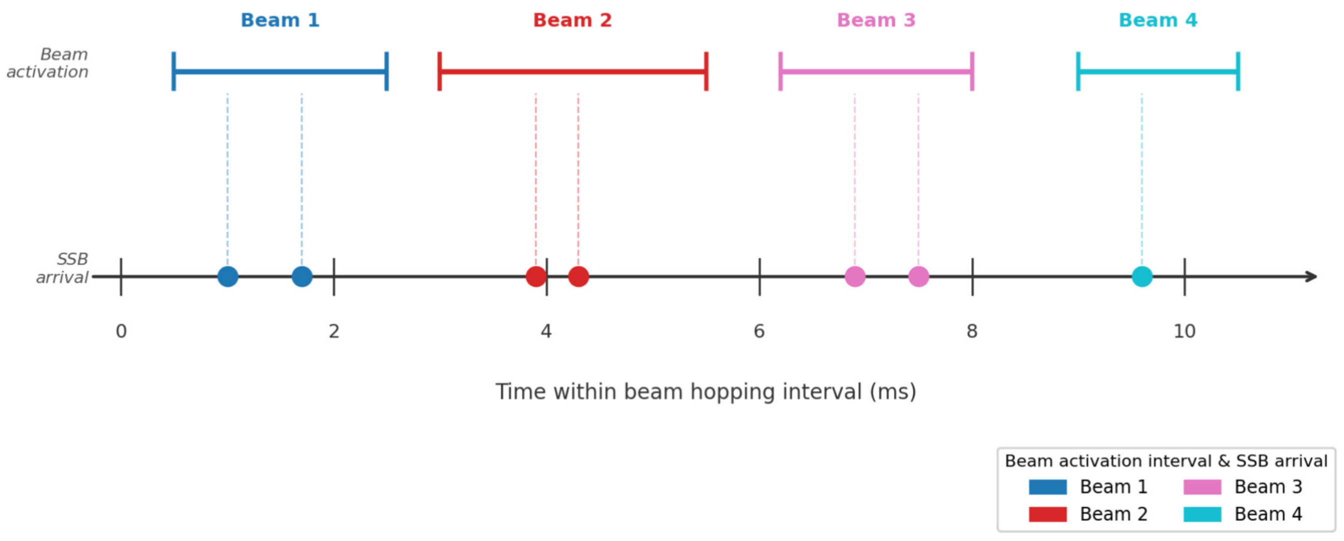


**FIGURE 1** | Beam hopping transmission concept.

each beam activation period, downlink signals, including SSBs, are transmitted toward the corresponding geographical region. Therefore, unlike nonhopped operation, the SSB transmission time associated with a beam depends on its position in the hopping schedule. Figure 1 illustrates this operation, where multiple beams are activated sequentially within one hopping interval.

The SSB arrival time observed at the UE is determined by both the beam activation time and the propagation delay from the satellite to the UE. The latter depends on satellite geometry, beam location, and UE position [12]. As a result, two beams activated at nearby transmission times may still produce different arrival times at the UE if their propagation delays differ, whereas beams activated at separated transmission times may produce disjoint monitoring opportunities even when their propagation delays are similar. This combined effect is the main source of timing dispersion considered in this paper.

The spatial pattern of beam hopping further determines how such timing dispersion appears at the UE. Figure 2 shows two representative patterns. In clustered illumination, neighboring beams within a geographically compact region are activated within the same hopping cycle. Since these beams are spatially close, their propagation delay differences are relatively small, and their SSB arrivals tend to form a small number of timing regions. In scattered illumination, beams serving geographically separated regions are activated within the same cycle. The propagation delay differences and activation-time separation can then be larger, causing SSB arrivals to be distributed across a wider portion of the hopping interval.

From the UE perspective, the resulting SSB arrivals are not necessarily distributed continuously over the entire hopping interval. Instead, beams with similar activation and propagation-delay characteristics may form distinct timing regions that can each be monitored by one SMTC window. This observation motivates the illumination-group abstraction introduced in Section 3, where the required number of SMTC configurations is related to the number of distinct timing groups observed by the UE.

## 2.3 | Related Work

Synchronization in satellite and NTN systems has been studied mainly from the physical-layer perspective. Kim and Park proposed a robust symbol timing synchronization scheme for LEO initial access under the DVB-RCS2 standard, focusing on Doppler-induced errors in short-packet transmission [13]. Omri et al. analyzed the 5G NR synchronization procedure and its timing structure in terrestrial systems [11]. Elmahallawy et al. proposed an improved primary synchronization signal detector for NTN handheld devices with Doppler compensation [14]. These studies improve or analyze synchronization signal detection under challenging channel conditions, but they do not address how beam hopping changes the SMTC monitoring window requirements.

Beam hopping has also been investigated from scheduling and resource allocation perspectives. Tang et al. studied resource allocation for LEO beam-hopping satellites in spectrum-sharing scenarios [15], and Ding et al. considered beam-hopping–based resource allocation in integrated satellite-terrestrial networks [16]. Zhang et al. evaluated beam hopping in an NR-based LEO system and examined the relationship between SSB period length and initial access delay [17]. Lv et al. studied beam position design for low-latency LEO satellite systems with beam hopping [18]. These works demonstrate the importance of beam hopping for efficient resource utilization, but the resulting UE-side SMTC configuration problem remains largely unaddressed.

At the standardization level, 3GPP TR 38.821 and TS 38.213 provide the baseline NR-NTN assumptions and SMTC configuration framework used in this paper [5, 10]. Recent work on earth-fixed beam management for 3GPP NTN common signalling has considered beam layout and hopping-pattern design for common signalling coverage [19]. However, the interaction between beam hopping timing dispersion and the limited number of SMTC monitoring windows has not been explicitly characterized.

This paper complements the above studies by focusing on the timing-domain monitoring problem induced by beam hopping. Rather than modifying the physical-layer SSB detector or optimizing the beam hopping scheduler itself, we analyze how beam



15420981, 0, Downloaded from https://onlinelibrary.wiley.com/doi/10.1002/sat.70073 by Hee Wook Kim - Electronics and Telecommunications , Wiley Online Library on [09/07/2026]. See the Terms and Conditions (https://onlinelibrary.wiley.com/terms-and-conditions) on Wiley Online Library for rules of use; OA articles are governed by the applicable Creative Commons License

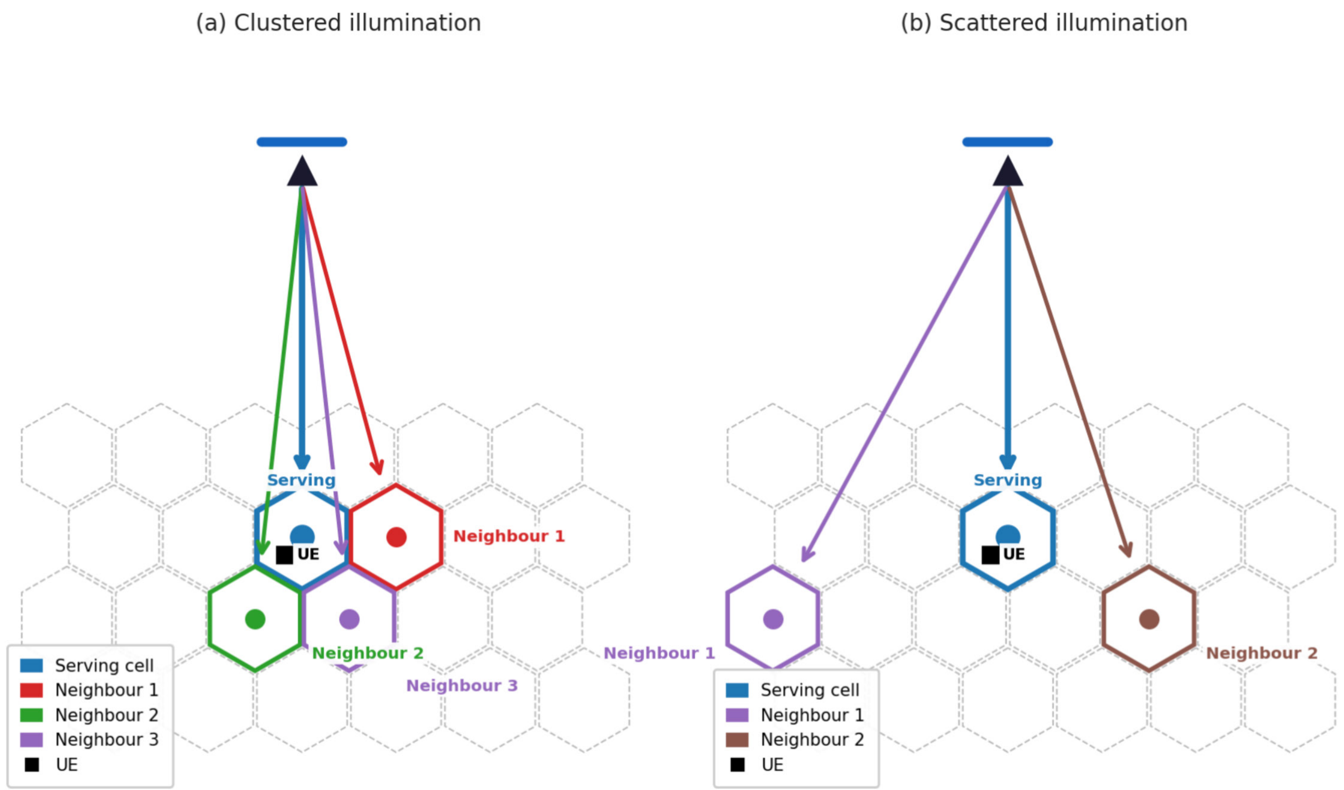


**FIGURE 2** | Clustered and scattered beam hopping patterns.

hopping creates multiple SSB timing groups at the UE, how the current SMTC constraint affects monitoring coverage, and how location-based configuration selection and adaptive window adjustment can mitigate the resulting monitoring loss. This positioning also provides the basis for the system-level and standardization discussions developed in the following sections.

## 3 | Limitation of the Existing SMTC Configuration Mechanism

Section 2 showed that beam hopping can distribute SSB arrival opportunities over multiple separated timing regions. This section quantifies how this behavior interacts with the limited number of SMTC configurations supported by the current NR framework. The analysis focuses on timing-domain monitoring success, i.e., whether the relevant SSB arrival falls inside an activated monitoring window. Link-level effects such as fading, interference, and false-alarm probability are outside the scope of this section and can be incorporated as additional conditional detection factors.

Let $\tau = \{\tau_1, \tau_2, \ldots, \tau_N\}$ denote the set of SSB arrival times observed by the UE within one beam hopping interval, where $N$ is the number of relevant serving or neighboring beams and $\tau_i$ is the arrival time of the SSB associated with the $i$-th beam. The overall timing spread is

$$\Delta\tau = \max_i \tau_i - \min_i \tau_i, \quad (1)$$

which gives the total temporal extent of the SSB arrival opportunities. If arrivals were continuously distributed over this interval, the minimum number of monitoring windows required to cover the whole spread would be

$$N_{\mathrm{SMTC}}^{\mathrm{cov}} = \left\lceil \frac{\Delta\tau}{W} \right\rceil, \quad (2)$$

where $W$ is the SMTC window duration.

In beam hopping systems, however, SSB arrivals are typically not continuous over $\Delta\tau$. Beams that are activated at similar instants and have similar propagation delays may generate arrivals that can be covered by the same monitoring window. We therefore define a timing group as a set of SSB arrivals that can be captured by one SMTC monitoring window of duration $W$, including the required timing margin. Let $G_s$ denote the number of such groups observed by the UE under illumination scenario $s \in \{7\mathrm{C}, 4\mathrm{C}, 3\mathrm{C}, 2\mathrm{C}, \mathrm{SC}\}$, corresponding to the seven-clustered, four-clustered, three-clustered, two-clustered, and scattered configurations. The required number of SMTC configurations for timing coverage is then

$$N_{\mathrm{SMTC},s}^{\mathrm{req}} = G_s. \quad (3)$$

This expression reflects the structured nature of beam hopping: The monitoring requirement is determined by the number of distinct timing groups rather than by the continuous timing spread alone. In general, $G_s \le N_{\mathrm{SMTC}}^{\mathrm{cov}}$ because the SSB arrivals are grouped according to the illumination pattern instead of filling the entire timing interval.

Figure 3 illustrates representative clustered illumination cases. Even when beams are activated in geographically adjacent regions, the number of timing groups observed by a boundary UE



15420981, 0, Downloaded from https://onlinelibrary.wiley.com/doi/10.1002/sat.70073 by Hee Wook Kim - Electronics and Telecommunications , Wiley Online Library on [09/07/2026]. See the Terms and Conditions (https://onlinelibrary.wiley.com/terms-and-conditions) on Wiley Online Library for rules of use; OA articles are governed by the applicable Creative Commons License

depends on the relative timing among the serving and neighboring beam activations. In the seven-clustered–cell case in Figure 3a, the arrivals can be covered by three monitoring windows, giving $G_s = 3$. As the cluster size decreases, the arrival opportunities become more fragmented. The four-, three-, and two-clustered–cell cases in Figure 3b–d therefore require $G_s = 4$, $G_s = 5$, and $G_s = 6$ timing groups, respectively. This shows that the required number of SMTC configurations is not determined solely by the number of simultaneously illuminated beams, but by the timing relationship of the SSB arrivals as observed at the UE.

Scattered illumination can further increase $G_s$. Figure 4 shows two representative scattered patterns. In randomly scattered illumination, beams serving geographically separated regions may be activated with largely independent timing relationships, producing up to $G_s = 7$ timing groups. Group-based scattered illumination can reduce timing dispersion by coordinating the activation order within predefined groups. Nevertheless, the number of timing groups can still exceed the four SMTC configurations supported by the current NR framework.

Let $M$ denote the number of SMTC configurations that can be activated by the UE. Under the current constraint, $M = 4$. If the relevant timing group is assumed to be uniformly distributed among the $G_s$ groups, the probability that this group is included in the activated monitoring set is

$$P_{\text{grp},s} = \frac{\min(M, G_s)}{G_s}. \tag{4}$$

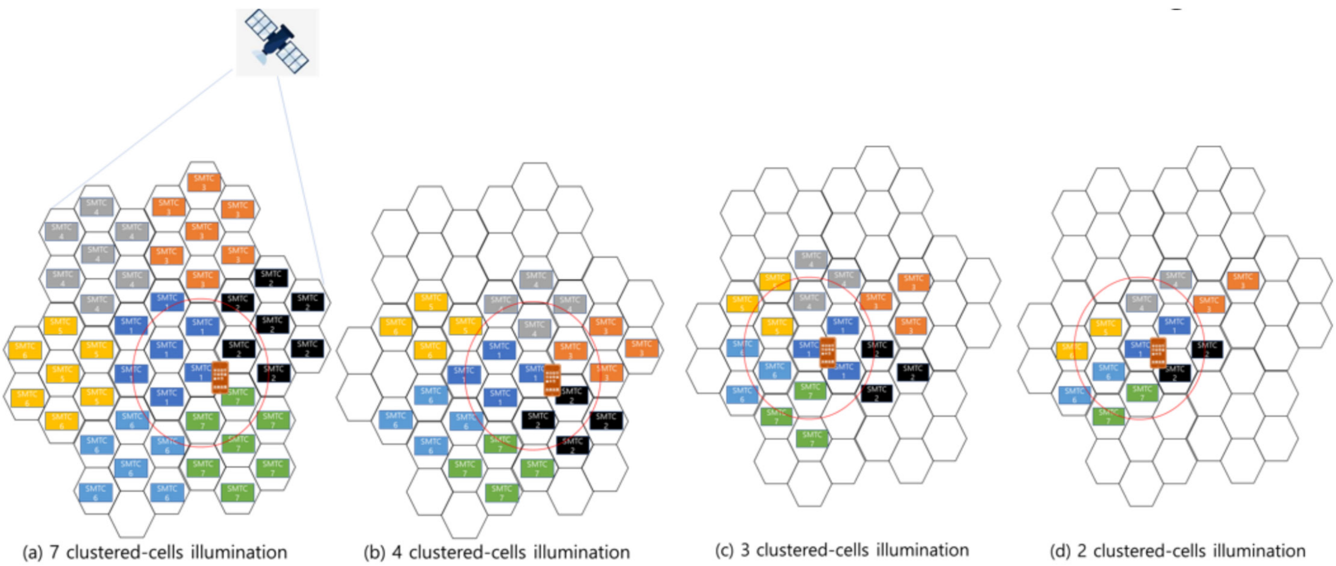


**FIGURE 3** | Required SMTC monitoring windows under clustered beam hopping illumination: (a) 7-cell, (b) 4-cell, (c) 3-cell, and (d) 2-cell configurations.

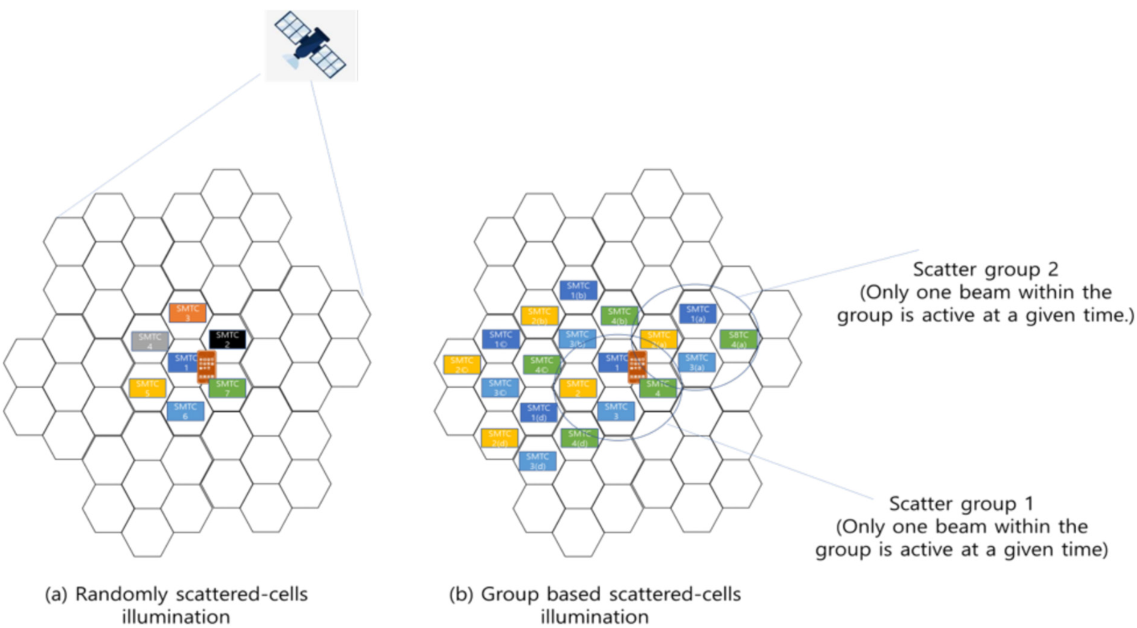


**FIGURE 4** | Scattered beam hopping illumination patterns: (a) randomly scattered and (b) group-based scattered illumination.



15420981, 0, Downloaded from https://onlinelibrary.wiley.com/doi/10.1002/sat.70073 by Hee Wook Kim - Electronics and Telecommunications , Wiley Online Library on [09/07/2026]. See the Terms and Conditions (https://onlinelibrary.wiley.com/terms-and-conditions) on Wiley Online Library for rules of use; OA articles are governed by the applicable Creative Commons License

This uniform assumption provides a tractable baseline for analyzing the effect of the SMTC configuration limit. In practical deployments, different groups may have different priorities depending on serving beam association, neighbor-cell ranking, traffic demand, or mobility state. Such priority weights can be incorporated by replacing (4) with a weighted sum over the activated timing groups, without changing the two-stage structure of the analysis.

The group-coverage probability captures only whether the correct timing group is monitored. Even when the group is selected, the SSB arrival may fall outside the monitoring window if the window is not aligned with the actual arrival time at the UE.

For beam g, let $t_g$ denote the nominal SSB arrival time at the corresponding beam reference point:

$$t_g = t_g^{\mathrm{tx}} + \frac{\| \mathbf{r}_{\mathrm{sat}}(t_g^{\mathrm{tx}}) - \mathbf{p}_g \|}{c}, \tag{5}$$

where $t_g^{\mathrm{tx}}$ is the satellite transmission time, $\mathbf{r}_{\mathrm{sat}}(t) \in \mathbb{R}^3$ denotes the satellite position vector at time $t$ in a common coordinate system, $\mathbf{p}_g \in \mathbb{R}^3$ is the beam reference-point position vector, and $c$ is the speed of light. For a UE located at $\ell$, the differential propagation delay between the beam reference point and the UE is

$$d_g = \frac{\| \mathbf{r}_{\mathrm{sat}}(t_g^{\mathrm{tx}}) - \ell \|}{c} - \frac{\| \mathbf{r}_{\mathrm{sat}}(t_g^{\mathrm{tx}}) - \mathbf{p}_g \|}{c}. \tag{6}$$

The actual SSB arrival time at the UE is then

$$\tau_g = t_g + d_g + \xi_g, \tag{7}$$

where $\xi_g$ represents residual timing uncertainty caused by satellite motion and scheduling update latency. If the satellite position used for scheduling is updated every $\Delta t_{\mathrm{sch}}$, a first-order approximation gives

$$|\xi_g| \approx \frac{\| \dot{\mathbf{r}}_{\mathrm{sat}}(t_g^{\mathrm{tx}}) \| \, \Delta t_{\mathrm{sch}}}{c}. \tag{8}$$

Here, $\dot{\mathbf{r}}_{\mathrm{sat}}(t) = d\mathbf{r}_{\mathrm{sat}}(t)/dt$ denotes the satellite velocity vector at time $t$, and $\| \dot{\mathbf{r}}_{\mathrm{sat}}(t) \|$ represents the satellite speed. For a representative LEO velocity of 7.5 km/s and $\Delta t_{\mathrm{sch}} = 100$ ms, this term is approximately 2. 5 μs. It is therefore much smaller than the millisecond-level differential propagation delay considered below, although it is kept in the model to represent scheduling uncertainty and multisatellite operation.

The timing offset between the nominal monitoring window center and the actual SSB arrival is

$$\epsilon_g = \tau_g - t_g = d_g + \xi_g. \tag{9}$$

The dominant component is $d_g$, whose magnitude depends on the UE position within the beam and the elevation angle. Using a beam radius of $R_{\mathrm{beam}} = 200$ km, consistent with the simulation configuration in Section 5, the maximum differential delay can be approximated by

$$d_g^{\max} \approx \frac{R_{\mathrm{beam}}}{c \sin \theta_{\min}} = \frac{200\ \mathrm{km}}{3 \times 10^5\ \mathrm{km/s} \times \sin 10^\circ} \approx 3.84\ \mathrm{ms}, \tag{10}$$

where $\theta_{\min}$ is the minimum elevation angle. Since this value exceeds the representative SMTC window duration of $W = 2$ ms, a window centered only at the beam reference-point arrival time may fail to capture the actual arrival for UEs near the beam edge, especially at low elevation angles.

The alignment probability for beam $g$ is therefore

$$P_{\mathrm{align}}(g) = \Pr\left[|\epsilon_g| \le \frac{W}{2}\right] = \Pr\left[|d_g + \xi_g| \le \frac{W}{2}\right]. \tag{11}$$

Combining timing-group coverage and window alignment, the SMTC monitoring success probability for scenario $s$ can be expressed as follows:

$$P_{\mathrm{mon},s} = P_{\mathrm{grp},s}\, P_{\mathrm{align},s}, \tag{12}$$

where $P_{\mathrm{align},s}$ denotes the average probability that the SSB arrival of a monitored timing group falls within the corresponding SMTC window. Therefore, $P_{\mathrm{mon},s}$ represents the probability that a relevant SSB monitoring opportunity is captured by an active SMTC window. Link-level effects, such as fading, interference, receiver implementation, and detection thresholds, affect the subsequent SSB detection or decoding probability and are outside the timing-domain monitoring scope of this paper.

A straightforward way to increase $P_{\mathrm{grp},s}$ is to activate more SMTC configurations. However, doing so directly increases the UE monitoring duty cycle:

$$\delta = \frac{MW}{T_h}, \tag{13}$$

where $T_h$ is the beam hopping interval. With $W = 2$ ms and $T_h = 20$ ms, increasing $M$ from 4 to 7 raises $\delta$ from 40% to 70%. This is a non-negligible overhead for power-constrained handheld and IoT-type NTN devices.

The above analysis identifies two distinct limitations of the current SMTC framework under beam hopping operation. First, when $G_s > M$, a coverage limitation occurs because not all timing groups can be monitored. Second, even when the relevant group is monitored, timing misalignment may occur because the actual SSB arrival at the UE is shifted from the nominal beam reference-point timing by $\epsilon_g = d_g + \xi_g$. The enhanced framework in Section 4 addresses these two limitations separately: Location-based configuration selection improves timing-group coverage, whereas adaptive window adjustment improves alignment with the actual SSB arrival time.

## 4 | Enhanced SMTC Monitoring Framework for Beam Hopping NTN

The analysis in Section 3 identified two limitations of the current SMTC framework under beam hopping operation. The first is a coverage limitation: When the number of timing groups $G_s$ exceeds the number of active SMTC configurations $M$, some SSB arrival opportunities are not monitored. The second is a timing-alignment limitation: Even if the relevant timing group is monitored, the actual arrival time at the UE may be shifted from the nominal monitoring window center by $\epsilon_g = d_g + \xi_g$. This



15420981, 0, Downloaded from https://onlinelibrary.wiley.com/doi/10.1002/sat.70073 by Hee Wook Kim - Electronics and Telecommunications , Wiley Online Library on [09/07/2026]. See the Terms and Conditions (https://onlinelibrary.wiley.com/terms-and-conditions) on Wiley Online Library for rules of use; OA articles are governed by the applicable Creative Commons License

section proposes an enhanced SMTC monitoring framework that addresses these limitations through two complementary functions: location-based configuration selection and adaptive window adjustment.

The proposed framework separates network-side configuration management from UE-side activation. The network may maintain a candidate pool of SMTC configurations covering the timing patterns expected across the satellite footprint, whereas each UE activates only a capability-limited subset relevant to its location and monitoring needs. The selected windows are then adjusted, when sufficient timing assistance is available, to better align with the estimated SSB arrival time at the UE. This structure improves timing-domain monitoring performance without requiring all candidate configurations to be simultaneously activated.

## 4.1 | Location-Based SMTC Configuration Strategy

### 4.1.1 | Design Principle

As shown in Section 3, the number of required monitoring windows depends on the timing groups observed by the UE. Since these groups are determined by the beam hopping schedule, satellite geometry, and UE location, a fixed SMTC configuration set may be inefficient across the entire satellite footprint. A UE near a region where several beam activation timings are separated may require more candidate windows than a UE located in a region where arrivals are temporally clustered.

To address this spatial dependency, the network maintains a candidate configuration pool $\{(c_j, \mathbf{p}_j)\}_{j=1}^{N_{\text{pool}}}$, where $c_j$ denotes an SMTC configuration and $\mathbf{p}_j$ denotes the reference location or reference region associated with that configuration. The pool size is chosen such that $N_{\text{pool}} \geq \max_s G_s$ for the considered beam hopping operation. The UE does not activate all candidate configurations. Instead, it selects at most $M$ configurations according to its UE capability and monitoring requirement, thereby keeping the duty cycle $\delta = MW/T_h$ bounded.

A low-complexity implementation is nearest reference selection, in which the UE activates the configurations whose reference locations are closest to its estimated position $\ell$:

$$\mathcal{S} = \underset{\mathcal{A}\subseteq\{1,\dots,N_{\text{pool}}\},\ |\mathcal{A}|\leq M}{\operatorname{argmin}} \sum_{j\in\mathcal{A}} \|\ell - \mathbf{p}_j\|. \tag{14}$$

This rule is intended as a practical baseline. More generally, the selection metric may also include predicted timing-group coverage, serving or neighboring beam priority, expected received power, mobility state, and UE capability. Such extensions do not change the proposed architecture, because the essential principle is to select a UE-specific subset from a larger network-provided candidate pool.

### 4.1.2 | Idle and Inactive Mode Operation

In idle or inactive mode, the UE performs configuration selection autonomously using assistance information obtained from the NTN system. Figure 5 illustrates the procedure. The NTN gNB broadcasts the candidate SMTC configuration pool and its associated reference-location information through system information or NTN assistance information. The UE receives this information as part of the cell search and system information acquisition procedure, before full connection establishment. Therefore, the proposed operation does not require the UE to be connected to a terrestrial network before acquiring the NTN link.

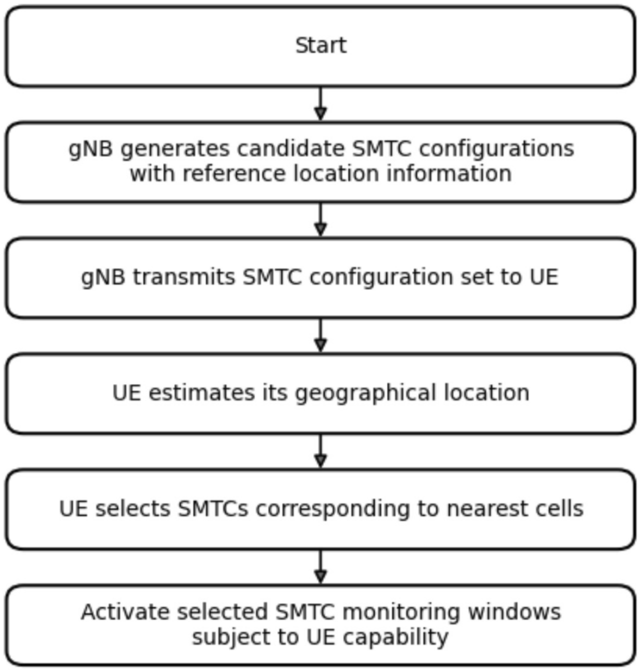


**FIGURE 5** | Location-based SMTC selection procedure in idle/inactive mode.

After obtaining the candidate pool, the UE estimates its position $\ell$ using GNSS or other available positioning assistance and selects a subset $\mathcal{S}$ according to (14). The UE then activates the selected monitoring windows subject to its simultaneous activation capability. When the UE moves, or when updated assistance information is received, the UE reevaluates the selection and updates the active configuration set.

If the assistance information is unavailable, outdated, or inconsistent with the detected NTN cell, the UE can fall back to legacy NR-NTN SMTC operation or to a conservative default configuration set indicated by the network. If the position estimate is temporarily unavailable or its uncertainty exceeds a configured threshold, the UE may use the last valid position estimate, select a broader subset of candidate configurations within its capability, or apply the window extension rule described in Section 4.2. These fallback modes preserve backward compatibility and provide graceful degradation when location or assistance information is degraded.

The idle/inactive-mode procedure is summarized in Algorithm 1.



15420981, 0, Downloaded from https://onlinelibrary.wiley.com/doi/10.1002/sat.70073 by Hee Wook Kim - Electronics and Telecommunications , Wiley Online Library on [09/07/2026]. See the Terms and Conditions (https://onlinelibrary.wiley.com/terms-and-conditions) on Wiley Online Library for rules of use; OA articles are governed by the applicable Creative Commons License

**ALGORITHM 1** | Location-based SMTC selection in idle/inactive mode.

**Input:** Candidate pool $\{(c_j, \mathbf{p}_j)\}_{j=1}^{N_{\text{pool}}}$, UE capability $M$
**Output:** Active SMTC configuration set $\mathcal{S}$
Receive candidate pool and reference-location information from NTN system information or assistance information
Obtain UE position estimate $\ell$ and its uncertainty
**if** assistance information is unavailable or invalid **then**
    Select legacy or conservative default SMTC configuration
    **return** $\mathcal{S}$
**end if**
**for** $j = 1$ to $N_{\text{pool}}$ **do**
    Compute selection metric for configuration $c_j$
**end for**
Select up to $M$ configurations according to the metric
Activate monitoring windows in $\mathcal{S}$
Upon position or assistance update, repeat the procedure

### 4.1.3 | Connected Mode Operation

In connected mode, the network can assist the selection using more accurate beam scheduling, ephemeris, and UE-context information, as illustrated in Figure 6. The UE may report a position estimate, a coarse location indicator, or the index of a reference region from the previously received pool. The gNB then determines the timing groups visible from the reported UE location based on the current beam hopping schedule, beam reference points, and satellite ephemeris.

The connected-mode procedure is also where network-side scheduling and gateway coordination are most relevant. In a typical NTN deployment, the beam hopping schedule is determined or updated by the satellite gateway or the RAN-side scheduler. The NTN gNB can use this schedule to construct or update the candidate SMTC pool and the mapping between reference regions and configurations. When the hopping schedule changes, the gNB updates the broadcast assistance information or delivers a UE-specific configuration through dedicated RRC signalling. This ensures that the UE-side monitoring configuration remains consistent with the active beam hopping schedule without requiring the UE to track the full scheduling state.

The connected-mode procedure is summarized in Algorithm 2.

## 4.2 | Adaptive SMTC Window Adjustment

The location-based strategy improves timing-group coverage by selecting the monitoring windows relevant to the UE. However,

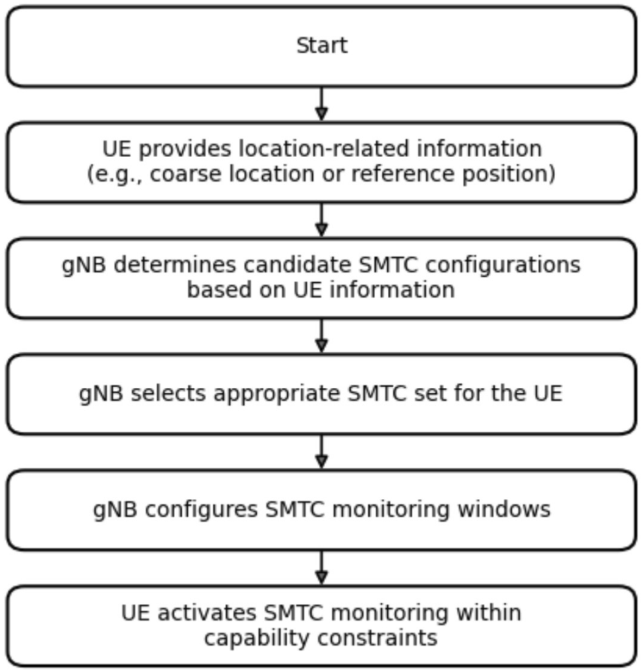


**FIGURE 6** | Location-based SMTC selection procedure in connected mode.

**ALGORITHM 2** | Network-assisted SMTC selection in connected mode.

**Input:** Beam hopping schedule $\{(b_i, t_i)\}$, beam reference points $\{\mathbf{p}_g\}$, UE location report $\ell$, UE capability $M$
**Output:** Active SMTC configuration set $\mathcal{S}$
UE reports location-related information to the NTN gNB
gNB identifies timing groups visible from $\ell$ using the beam hopping schedule and ephemeris
gNB maps the timing groups to candidate SMTC configurations
gNB selects up to $M$ configurations according to coverage and priority
gNB delivers $\mathcal{S}$ through dedicated RRC signalling
UE activates the configured monitoring windows
Upon UE movement or schedule update, repeat the procedure

coverage alone does not guarantee that the SSB arrival falls inside the selected window, because the actual arrival time may be shifted from the nominal beam reference-point timing by the differential propagation delay $d_g$. Under the $R_{\text{beam}} = 200$-km model used in Section 3, this offset can reach approximately 3.84 ms at low elevation angles, which exceeds the representative SMTC window duration of $W = 2$ ms. Window adjustment is therefore needed to improve alignment.

For beam $g$, the adjusted window center is set to the estimated SSB arrival time at the UE:



15420981, 0, Downloaded from https://onlinelibrary.wiley.com/doi/10.1002/sat.70073 by Hee Wook Kim - Electronics and Telecommunications , Wiley Online Library on [09/07/2026]. See the Terms and Conditions (https://onlinelibrary.wiley.com/terms-and-conditions) on Wiley Online Library for rules of use; OA articles are governed by the applicable Creative Commons License

$$\hat{\tau}_g = t_g + \hat{d}_g, \tag{15}$$

where $\hat{d}_g$ is the estimated differential propagation delay:

$$\hat{d}_g = \frac{\|\mathbf{r}_{\text{sat}}(t_g^{\text{tx}}) - \ell\|}{c} - \frac{\|\mathbf{r}_{\text{sat}}(t_g^{\text{tx}}) - \mathbf{p}_g\|}{c}. \tag{16}$$

This estimate can be computed by the gNB in connected mode using the reported UE position and satellite ephemeris, or by the UE in autonomous operation if the required assistance information is available.

The residual timing error after adjustment is

$$E_g = \tau_g - \hat{\tau}_g = (d_g - \hat{d}_g) + \xi_g = \tilde{d}_g + \xi_g, \tag{17}$$

where $\tilde{d}_g$ is the differential-delay estimation error. If the position uncertainty is $\sigma_\ell$, a first-order approximation gives

$$|\tilde{d}_g| \approx \frac{\sigma_\ell}{c \sin\theta_g}, \tag{18}$$

where $\theta_g$ is the elevation angle of beam g. For $\sigma_\ell = 10$ m, the residual error is approximately 66 ns at $\theta_g = 30°$ and approximately 190 ns at $\theta_g = 10°$. These values are much smaller than $W/2 = 1$ ms. Together with the scheduling uncertainty term $\xi_g$, this residual error determines the adjusted alignment probability:

$$P_{\text{align}}^{\text{adj}}(g) = \Pr\left[|\tilde{d}_g + \xi_g| \le \frac{W}{2}\right]. \tag{19}$$

When the position uncertainty becomes large, the adjusted window may be extended to preserve timing coverage:

$$W_g = W + 2\frac{\sigma_\ell}{c \sin\theta_g}. \tag{20}$$

This extension increases the monitoring duty cycle for the affected configuration but provides a controlled fallback under degraded positioning. The network or UE may apply the extension only when the estimated uncertainty exceeds a configured threshold, thereby balancing robustness and power consumption.

The combined procedure is summarized in Algorithm 3 and illustrated in Figure 7. The upper timing diagram corresponds to unadjusted operation, where the window remains centered at the nominal reference-point timing. The lower timing diagram shows adjusted operation, where the window is shifted toward the estimated arrival time at the UE.

**ALGORITHM 3** | Combined location-based selection and adaptive window adjustment.

**Input:** Active configuration set $\mathcal{S}$, beam reference points $\{\mathbf{p}_g\}$, UE position estimate $\ell$ and uncertainty $\sigma_\ell$, satellite ephemeris $\mathbf{r}_{\text{sat}}(\cdot)$, nominal reference-point arrival times $\{t_g\}$

**Output:** Adjusted SMTC configuration set $\mathcal{S}^{\text{adj}}$

1: **for** each configuration in $\mathcal{S}$ associated with beam g **do**
2: Compute $\hat{d}_g$ using (16)
3: Set adjusted window centre $\hat{\tau}_g \leftarrow t_g + \hat{d}_g$
4: **if** $\sigma_\ell/(c\sin\theta_g)$ exceeds the configured threshold **then**
5: Extend the window duration according to (20)
6: **end if**
7: **end for**
8: Activate the adjusted monitoring windows

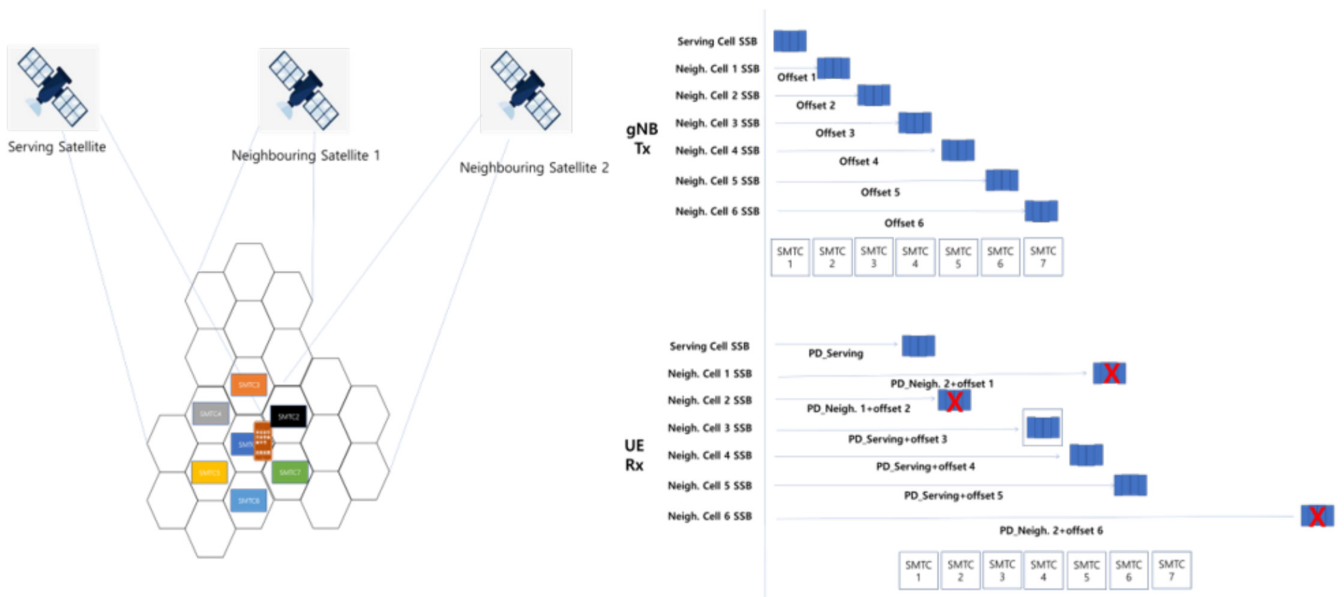


**FIGURE 7** | Concept of adaptive SMTC window adjustment in beam hopping NTN systems.



15420981, 0, Downloaded from https://onlinelibrary.wiley.com/doi/10.1002/sat.70073 by Hee Wook Kim - Electronics and Telecommunications , Wiley Online Library on [09/07/2026]. See the Terms and Conditions (https://onlinelibrary.wiley.com/terms-and-conditions) on Wiley Online Library for rules of use; OA articles are governed by the applicable Creative Commons License

With location-based selection and adaptive adjustment, the monitoring success probability becomes

$$P_{\mathrm{mon},s}^{(2)} = P_{\mathrm{grp},s}^{(2)} P_{\mathrm{align},s}^{\mathrm{adj}}, \tag{21}$$

where $P_{\mathrm{grp},s}^{(2)}$ reflects the selected timing-group coverage and $P_{\mathrm{align},s}^{\mathrm{adj}}$ is the average adjusted alignment probability over the monitored groups. When the candidate pool covers all relevant timing groups and the UE capability allows the required subset to be activated, $P_{\mathrm{grp},s}^{(2)} = 1$. Under sufficiently accurate position and ephemeris information, $P_{\mathrm{align},s}^{\mathrm{adj}}$ approaches unity in the timing-domain monitoring model. The resulting performance is evaluated in Section 5.

### 4.3 | Implementation and Standardization Considerations

The proposed framework preserves the basic SMTC timing semantics, since the UE still monitors SSBs within configured windows defined by periodicity, offset, and duration. However, practical implementation of beam-hopping-aware monitoring may require additional NTN assistance information. Such information may include candidate-pool indices, reference-location association, validity time, beam or illumination group identifiers, UE capability for simultaneous monitoring, and optional timing-adjustment information. These parameters can be introduced through system information or dedicated RRC signalling extensions in future NR-NTN evolution, while maintaining backward compatibility with UEs that support only baseline SMTC operation.

In idle or inactive mode, the candidate configuration pool and its associated reference-location information may be provided through broadcast assistance information. The UE can then select a capability-limited subset based on its location estimate without requiring prior connectivity to a terrestrial network. In connected mode, the serving NTN gNB can provide a UE-specific subset using more accurate knowledge of the UE location, beam hopping schedule, satellite ephemeris, and neighbor-beam timing relationships. This distinction allows the framework to support both autonomous UE-side operation and network-assisted optimization.

The framework also interacts naturally with network-side beam scheduling. In practical deployments, the beam hopping schedule may be determined or updated by the gateway or RAN-side scheduler according to traffic demand, satellite power constraints, coverage requirements, and service priorities. The NTN gNB can translate the active beam hopping schedule into a candidate SMTC configuration pool and update the reference-location mapping when the schedule changes. This separation prevents the UE from having to track the complete beam hopping schedule while still allowing the monitoring configuration to remain consistent with network-side scheduling decisions.

For mobility and multisatellite operation, candidate configurations can be associated with satellite- or beam-specific timing references. As the UE moves across reference regions or as the serving satellite changes, the active SMTC subset can be updated through autonomous reselection or dedicated signalling. The validity time of the assistance information can be used to determine when stored configuration information should be refreshed. If the assistance information is unavailable, stale, or inconsistent with the detected NTN cell, the UE can fall back to baseline NR-NTN SMTC operation or to a conservative default configuration set indicated by the network.

The framework also provides graceful degradation under degraded positioning conditions. If the UE position estimate is temporarily unavailable, the UE may use the last valid position estimate or select a broader subset of candidate configurations within its capability. If the position uncertainty is available but exceeds a configured threshold, the monitoring window duration can be extended according to (20), trading additional duty cycle for improved timing coverage. These fallback behaviors are particularly relevant for direct-to-device NTN terminals, where power consumption, positioning availability, and assistance-information validity may vary over time.

Overall, the proposed framework can be viewed as an enhancement to the NR-NTN measurement configuration procedure rather than a replacement of the existing SMTC mechanism. It retains the conventional notion of SMTC monitoring windows while adding beam-hopping-aware assistance and selection logic. This provides a practical migration path toward synchronization monitoring support for future beam hopping NR-NTN deployments.

## 5 | Performance Analysis

This section evaluates the proposed framework using Monte Carlo simulation based on the timing-domain model developed in Section 3. The objective is to quantify how timing-group coverage, window alignment, and monitoring duty cycle affect the probability that an SSB arrival opportunity is captured by an active SMTC window. Therefore, the performance metric is the SSB monitoring success probability, rather than the physical-layer decoding probability of the SSB. Channel fading, interference, and receiver detection thresholds can be incorporated as additional link-level factors, but are not the focus of this timing-domain evaluation.

To improve practical relevance, the simulation parameters are chosen based on representative NR-NTN deployment assumptions, following the system-level modelling perspective of 3GPP TR 38.821 [5]. The evaluation considers LEO satellite altitude, beam geometry, elevation-dependent propagation delay, SMTC window duration, and the beam hopping interval. The simulation parameters are summarized in Table 1. A LEO satellite altitude of 600 km and a beam radius of $R_{\mathrm{beam}} = 200$ km are used, consistent with the delay bound in (10). The serving beam is assumed to have an elevation angle of 30°. Neighboring beam regions are placed on a hexagonal grid, and their elevation angles are determined from their ground distances relative to the sub-satellite point. The beam hopping interval is $T_h = 20$ ms, and the nominal SMTC window duration is $W = 2$ ms.

Five illumination scenarios are considered: seven-clustered (7C), four-clustered (4C), three-clustered (3C), two-clustered (2C), and scattered (SC). These scenarios correspond to $G_s = 3, 4, 5, 6$, and 7, respectively, following the timing-group



15420981, 0, Downloaded from https://onlinelibrary.wiley.com/doi/10.1002/sat.70073 by Hee Wook Kim - Electronics and Telecommunications , Wiley Online Library on [09/07/2026]. See the Terms and Conditions (https://onlinelibrary.wiley.com/terms-and-conditions) on Wiley Online Library for rules of use; OA articles are governed by the applicable Creative Commons License

**TABLE 1** | Simulation parameters based on representative NR-NTN assumptions.

| Parameter | Value | Description |
|---|---|---|
| Satellite altitude | 600 km | LEO reference scenario |
| Beam radius $R_{\text{beam}}$ | 200 km | Radius used for delay and geometry model |
| Serving beam elevation | 30° | Reference serving-beam geometry |
| Beam hopping interval $T_h$ | 20 ms | One hopping cycle |
| SMTC window duration $W$ | 2 ms | Nominal monitoring window length |
| $G_s$ (7C/4C/3C/2C/SC) | 3/4/5/6/7 | Scenario-dependent timing groups |
| GNSS accuracy $\sigma_\ell$ | 10 m | Position uncertainty for B2 |
| Max. active SMTC (B0) | $M_0 = 4$ | Baseline NR constraint |
| Max. active SMTC (B1/B2) | $M_1 = M_2 = 7$ | Extended candidate support |
| Monte Carlo trials | $10^5$ | Statistical averaging |

structures illustrated in Figures 3, 4. For each scenario, the UE is assumed to be located near the edge of the serving region, where multiple timing groups may be relevant for synchronization monitoring.

For each group g, the differential propagation delay $d_g$ is generated according to the geometry in (6). To represent UE locations within the corresponding beam region, $d_g$ is modelled as uniformly distributed over $[d_g^{\min}, d_g^{\max}]$, where the bounds are determined by the beam radius and the elevation angle of the group. The residual scheduling uncertainty $\xi_g$ follows (8) and is much smaller than the millisecond-level differential delay. For B2, the residual delay after adaptive adjustment is determined by the position uncertainty according to (18).

The following three schemes are compared:

- **B0**: baseline NR SMTC operation with at most $M_0 = 4$ active configurations and no adaptive window adjustment.
- **B1**: location-based configuration extension with at most $M_1 = 7$ active configurations, but with windows still centered at the nominal reference-point timing.
- **B2**: the proposed combined scheme with location-based configuration selection and adaptive window adjustment.

In each Monte Carlo trial, a relevant timing group $g^*$ is drawn uniformly from the $G_s$ groups. This uniform selection isolates the effect of the SMTC configuration constraint. In practical deployments, the same evaluation can be extended by assigning non-uniform weights to timing groups according to serving-beam priority, neighbor-cell ranking, traffic load, or mobility state. A monitoring success event is declared if the selected group is included in the activated configuration set and the corresponding SSB arrival lies within the active monitoring window. For B0 and B1, the window is centered at the nominal reference-point timing; for B2, it is centered at the adjusted arrival estimate.

For scenario $s$ and scheme $k$, the monitoring success probability can be written as

$$P_{\text{mon},s}^{(k)} = \frac{1}{G_s} \sum_{g \in \mathcal{S}_k(s)} P_{\text{align}}^{(k)}(g), \tag{22}$$

where $\mathcal{S}_k(s)$ denotes the timing groups monitored under scheme $k$, with $|\mathcal{S}_k(s)| \leq \min(M_k, G_s)$. For B0 and B1, $P_{\text{align}}^{(k)}(g) = P_{\text{align}}(g)$ in (11). For B2, $P_{\text{align}}^{(k)}(g) = P_{\text{align}}^{\text{adj}}(g)$ in (19). Equation (22) is the per-group form of the monitoring success model in (12) and (21).

Figure 8 shows the monitoring success probability for the three schemes across the five illumination scenarios. The markers represent Monte Carlo results, and the lines represent the analytical prediction from (22). The analytical and simulation results closely match, confirming that the proposed illumination-group model captures the dominant timing-domain monitoring behavior.

Under B0, 7C and 4C do not suffer from timing-group coverage loss because $G_s \leq M_0$. Their monitoring success probability is therefore limited only by window misalignment. The 4C case may show a higher probability than the 7C case because the specific cluster directions included in the 4C scenario have elevation angles closer to the serving-beam reference elevation, which leads to smaller differential delay and higher alignment probability. This illustrates that the monitoring performance is determined jointly by the number of timing groups and the geometry-dependent alignment probability, rather than by $G_s$ alone.

For 3C, 2C, and SC, where $G_s > M_0$, B0 suffers from both coverage loss and timing misalignment. Some timing groups are not monitored because only four configurations can be activated, and the monitored groups may still experience differential-delay–induced window misalignment. As the illumination pattern becomes more fragmented, the coverage factor decreases and the monitoring success probability is further degraded.

B1 removes the coverage limitation by allowing up to seven active configurations. Therefore, all timing groups are monitored in the considered scenarios. However, the monitoring windows remain centered at the nominal reference-point timing, so the



15420981, 0, Downloaded from https://onlinelibrary.wiley.com/doi/10.1002/sat.70073 by Hee Wook Kim - Electronics and Telecommunications , Wiley Online Library on [09/07/2026]. See the Terms and Conditions (https://onlinelibrary.wiley.com/terms-and-conditions) on Wiley Online Library for rules of use; OA articles are governed by the applicable Creative Commons License

residual gap from unity is due to timing misalignment. This result confirms that merely increasing the number of SMTC configurations is insufficient when the actual SSB arrival time differs significantly from the nominal timing.

B2 combines the extended configuration support with adaptive window adjustment. Since the selected windows are shifted toward the estimated SSB arrival times, the residual timing error is dominated by position uncertainty and scheduling update error, both of which are small compared with $W/2$ under the assumed parameters. Consequently, B2 approaches unity monitoring success probability in the considered timing-domain model. This should be interpreted as an upper-bound timing-alignment result under accurate position and ephemeris assistance, rather than as a complete physical-layer SSB decoding probability.

To further clarify the role of geometry-dependent timing alignment, Figure 9 plots $P_{\text{align}}(g)$ as a function of beam elevation angle. The curve shows that the alignment probability is highest when the beam geometry is close to the reference serving-beam geometry and decreases when the elevation angle deviates from that reference. The scenario markers explain why some clustered cases do not follow a strictly monotonic trend with respect to $G_s$: The set of elevation angles included in each scenario also affects the average alignment probability.

Figure 10 illustrates the trade-off between monitoring success probability and duty cycle as the number of active SMTC configurations increases. The duty cycle is computed as $\delta = MW/T_h$. With $W = 2$ ms and $T_h = 20$ ms, the current configuration limit of $M = 4$ corresponds to $\delta = 40\%$, whereas activating seven

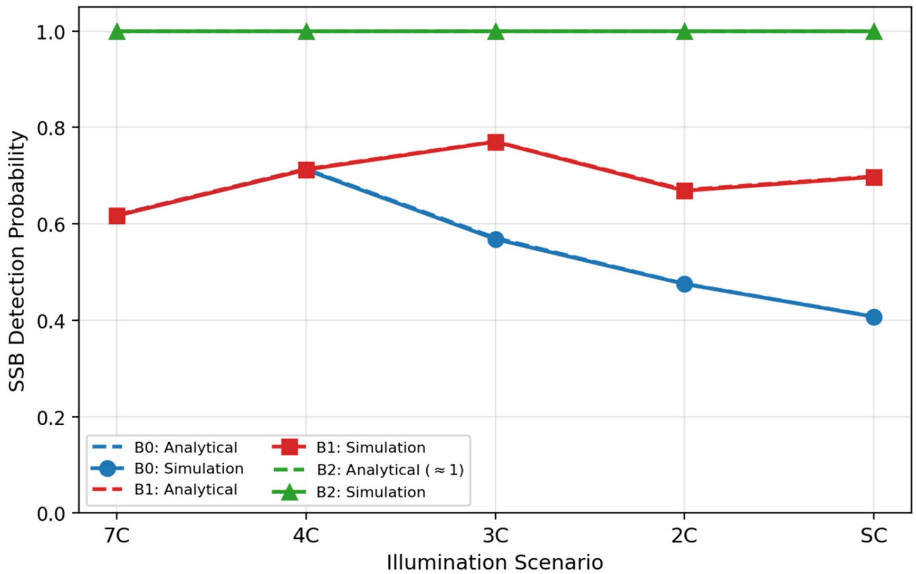


**FIGURE 8** | SSB monitoring success probability under B0 (baseline NR, $M_0 = 4$), B1 (location-based extension, $M_1 = 7$), and B2 (proposed, $M_2 = 7$ with adaptive window adjustment), with analytical predictions from (22).

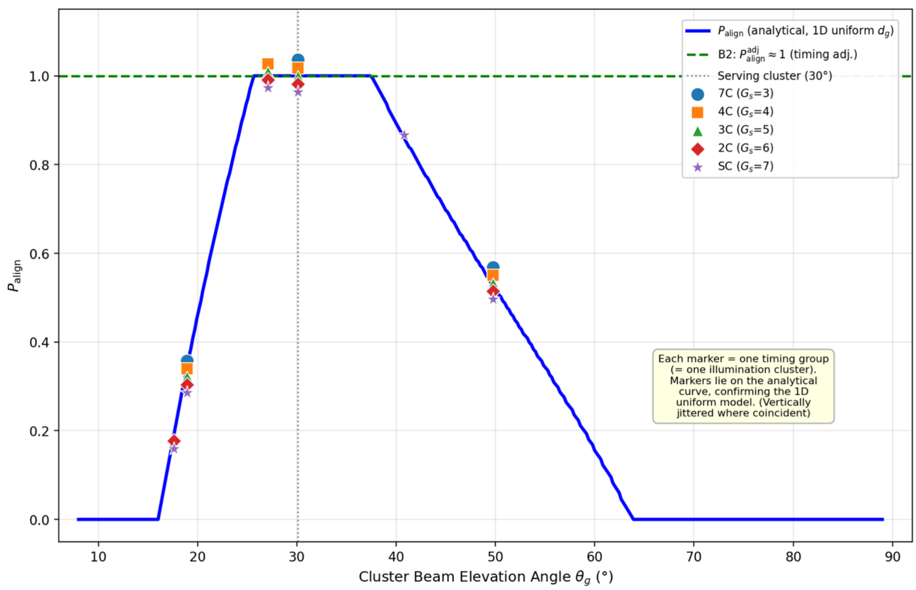


**FIGURE 9** | $P_{\text{align}}(g)$ as a function of beam elevation angle, with markers indicating the cluster directions used in each illumination scenario.



15420981, 0, Downloaded from https://onlinelibrary.wiley.com/doi/10.1002/sat.70073 by Hee Wook Kim - Electronics and Telecommunications , Wiley Online Library on [09/07/2026]. See the Terms and Conditions (https://onlinelibrary.wiley.com/terms-and-conditions) on Wiley Online Library for rules of use; OA articles are governed by the applicable Creative Commons License

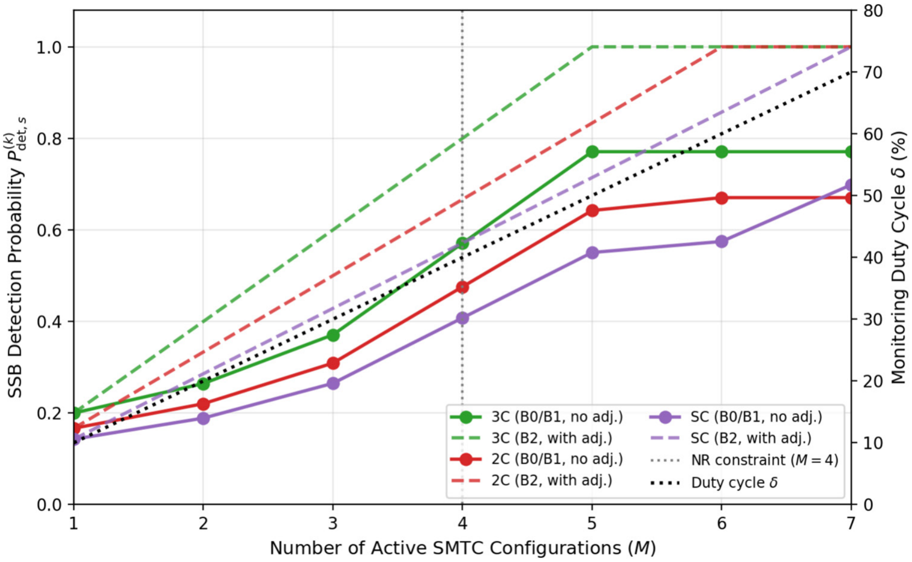


**FIGURE 10** | SSB monitoring success probability and monitoring duty cycle $\delta$ as a function of the number of active SMTC configurations $M$, for the 3C, 2C, and SC scenarios.

configurations corresponds to $\delta = 70\%$. Increasing $M$ improves timing-group coverage, especially for the 3C, 2C, and SC scenarios, but the gain saturates below unity without window adjustment because alignment loss remains. The proposed B2 scheme improves the monitoring success probability at the same configuration count as B1 by reducing the alignment loss rather than by increasing the number of active windows.

The results demonstrate that the two components of the proposed framework address different performance bottlenecks. Location-based configuration selection improves timing-group coverage by enabling the UE to select the configurations relevant to its position from a larger candidate pool. Adaptive window adjustment then improves the alignment of the selected monitoring windows with the actual SSB arrival times. The combined framework therefore provides a practical trade-off between monitoring performance and UE duty cycle, which is important for power-constrained direct-to-device and IoT-oriented NTN terminals.

## 6 | Conclusions

This paper investigated the timing-domain synchronization monitoring problem in beam hopping NR-NTN systems. The analysis showed that SSB arrival opportunities may be distributed across multiple distinct timing groups, and that the required number of SMTC configurations is therefore governed by the number of illumination groups observed by the UE. In the considered clustered and scattered beam hopping scenarios, this number ranges from three to seven, which may exceed the current NR SMTC configuration constraint. The proposed framework addresses the resulting monitoring limitation through two complementary mechanisms. The location-based SMTC configuration strategy allows the network to maintain a candidate configuration pool while enabling the UE to activate only a capability-limited subset relevant to its location. The adaptive window adjustment mechanism then shifts the selected monitoring windows toward the estimated SSB arrival times, thereby reducing the impact of differential propagation delay and scheduling uncertainty. Simulation results showed that the proposed framework improves SSB monitoring success probability across clustered and scattered illumination scenarios and clarifies the trade-off between monitoring performance and UE duty cycle. The results also indicate that configuration extension alone is insufficient when window misalignment remains, whereas the combined use of location-based selection and timing-aware adjustment can substantially improve timing-domain monitoring reliability. These findings provide practical design insights for beam-hopping-aware SMTC operation in future NR-NTN and direct-to-device satellite deployments.


### Funding

This work was supported by the ETRI R&D Program under Grant 26CH1110.


### Conflicts of Interest

The authors declare no conflicts of interest.

### References


1. M. Giordani and M. Zorzi, "Non-Terrestrial Networks in the 6G Era: Challenges and Opportunities," *IEEE Network* 35, no. 2 (2021): 244–251, https://doi.org/10.1109/MNET.011.2000493.

2. X. Lin, S. Rommer, S. Euler, E. A. Yavuz, and R. S. Karlsson, "5G From Space: An Overview of 3GPP Non-Terrestrial Networks," *IEEE Communications Standards Magazine* 5, no. 4 (2021): 147–153, https://doi.org/10.1109/MCOMSTD.101.2000059.

3. W. Saad, M. Bennis, and M. Chen, "A Vision of 6G Wireless Systems: Applications, Trends, Technologies, and Open Research Problems," *IEEE Network* 34, no. 3 (2020): 134–142, https://doi.org/10.1109/MNET.001.1900287.





15420981, 0, Downloaded from https://onlinelibrary.wiley.com/doi/10.1002/sat.70073 by Hee Wook Kim - Electronics and Telecommunications , Wiley Online Library on [09/07/2026]. See the Terms and Conditions (https://onlinelibrary.wiley.com/terms-and-conditions) on Wiley Online Library for rules of use; OA articles are governed by the applicable Creative Commons License

4. G. Araniti, A. Iera, S. Pizzi, and F. Rinaldi, "Toward 6G Non-Terrestrial Networks," *IEEE Network* 36, no. 1 (2022): 113–120, https://doi.org/10.1109/MNET.008.2100200.

5. 3GPP. "Solutions for NR to Support Non-Terrestrial Networks (NTN) (Release 16)," Technical Report TR 38.821, 3rd Generation Partnership Project; 2023. Version 16.2.0.

6. J. Kim, G. Casati, N. Cassiau, et al., "Design of Cellular, Satellite, and Integrated Systems for 5G and Beyond." *ETRI Journal* 42, no. 5 (2020): 669–685, https://doi.org/10.4218/etrij.2020-0221.

7. J. Anzalchi, A. Couchman, P. Gabellini, G. Gallinaro, L. D'Agristina, and N. Alagha, "Beam Hopping in Multi-Beam Broadband Satellite Systems: System Simulation and Performance Comparison With Non-Hopped Systems," in *ASMS-SPSC2010 Conference* (IEEE, 2010).

8. J. Lei and M. Á. Vázquez-Castro, "Multibeam Satellite Frequency/Time Duality Study and Capacity Optimization," *Journal of Communications and Networks* 13, no. 5 (2011): 472–480, https://doi.org/10.1109/JCN.2011.6157458.

9. R. Mu, C. Hu, Z. Hu, and Y. Li, "Dynamic Beam Hopping for LEO Satellites With Differentiated Traffic Demands," in *In 2023 International Conference on Wireless Communications and Signal Processing (WCSP)* (IEEE, 2023), 621–626.

10. 3GPP. "NR; Physical Layer Procedures for Control (Release 18)," Technical Specification TS 38.213, 3rd Generation Partnership Project; 2025. Version 18.8.0.

11. A. Omri, M. Shaqfeh, A. Ali, and H. Alnuweiri, "Synchronization Procedure in 5G NR Systems," *IEEE Access* 7 (2019): 41286–41295, https://doi.org/10.1109/ACCESS.2019.2907970.

12. H. W. Kim, K. Kang, B. J. Ku, D. I. Chang, and S. Kim, "SAT-OFDM: A Satellite Radio Interface for the IMT-Advanced System," *International Journal of Satellite Communications and Networking* 33, no. 4 (2015): 295–314, https://doi.org/10.1002/sat.1103.

13. P. Kim and H. Park, "Robust Symbol Timing Synchronization for Initial Access Under LEO Satellite Channel," *Sensors* 23, no. 19 (2023): 8320, https://doi.org/10.3390/s23198320.

14. R. Tuninato and R. Garello, "5G NTN Primary Synchronization Signal: An Improved Detector for Handheld Devices," *IEEE Open Journal of the Communications Society* 5 (2024): 3792–3803, https://doi.org/10.1109/OJCOMS.2024.3416554.

15. J. Tang, D. Bian, G. Li, J. Hu, and J. Cheng, "Resource Allocation for LEO Beam-Hopping Satellites in a Spectrum Sharing Scenario," *IEEE Access* 9 (2021): 56468–56478, https://doi.org/10.1109/ACCESS.2021.3071632.

16. F. Ding, C. Bao, D. Zhou, M. Sheng, Y. Shi, and J. Li, "Beam-Hopping-Based Resource Allocation in Integrated Satellite-Terrestrial Networks," *Sensors* 24, no. 14 (2024): 4699, https://doi.org/10.3390/s24144699.

17. J. Zhang, D. Qin, C. Kong, et al., "System-Level Evaluation of Beam Hopping in NR-Based LEO Satellite Communication System," in *In 2023 IEEE Wireless Communications and Networking Conference (WCNC)* (IEEE, 2023), 1–6.

18. L. Lv, C. Qi, and F. C. Zheng, "Beam Position Design for Low-Latency LEO Satellite Communications With Beam Hopping," in *In 2023 IEEE 24th International Workshop on Signal Processing Advances in Wireless Communications (SPAWC)* (IEEE, 2023), 321–325.

19. X Artiga, M Caus, and A Pérez-Neira, "Pragmatic Earth-Fixed Beam Management for 3GPP NTN Common Signaling in LEO Satellites," arXiv Preprint arXiv:2512.14368; 2025.



15420981, 0, Downloaded from https://onlinelibrary.wiley.com/doi/10.1002/sat.70073 by Hee Wook Kim - Electronics and Telecommunications , Wiley Online Library on [09/07/2026]. See the Terms and Conditions (https://onlinelibrary.wiley.com/terms-and-conditions) on Wiley Online Library for rules of use; OA articles are governed by the applicable Creative Commons License